Mansoura Engineering Journal

Volume 34 | Issue 2 Article 3

6-1-2021

Study of Turbulent Structure and Flow Characteristics through Inclined Finite Depression in Sloping Open Channel.

M. Attia

Associate Professor., Water & Water Structures Engineering Department., Faculty of Engineering., Zagazig University., Zagazig., Egypt.

A STUDY OF TURBULENT STRUCTURE AND FLOW CHARACTERISTICES THROUGH INCLNED FINITE DEPRESSION IN SLOPING OPEN CHANNEL

دراسة تكوين السريان المضطرب وخصائص الجريان خلال الإنخفاضات المائلة المحددة في قنوات مفتوحة منحدرة

M.I.ATTIA

Assoc. prof. Water & Water Structures Engg . Dept.

Faculty of Engg . , Zagazig University , Zagazig , Egypt.

ملخص: يهدف هذا البحث لدراسة معملية الجريان المضطرب وخصائص السريان خلال الإنخفاضات المحددة الطول وبأطوال مختلفة لطول نسبي (L/b) مقداره ٥ ، ١٠ ، ١٥ ، ٢٠ ، ٢٥ ، ٣٠ والمائلة بزوايا ميل مختلفة عند المدخل والمخرج في القنوات المستطيلة ذات الميول مختلفة. ويهتم الجزء الأول من البحث بدراسة خصائص الجريان المضطرب باستخدام جهاز الليزر لقياس مركبات سرعات الاضطراب للجريان وهي كثافات الاضطراب والسرعات المتوسطة في جميع الإتجاهات في اتجاه السريان والعمودي عليه وذلك لقطاعات عرضية مختلفة داخل الانخفاض وبعده في اتجاه عمق المياه. وتم عمل دراسة مقارنة للمتغيرات المختلفة للجريان المضطرب (كثافات الاضطراب والسرعات) عند قطاعات عرضية مختلفة لزوايا ميل مختلفة لمدخل ومخرج الانخفاض وهي ١٠° ، ١٥° ، ٢٠° ، ٢٥° ، ٣٠° ، ٩٠° . وكذلك دراسة مقارنة للقيم القصوى لمتغيرات السريان المضطرب في الاتجاه الطولي (في اتجاه محور القناه) داخل الانخفاض وبعده عند زوايا ميل مختلفة (١٥° ، ٤٥° ، ٩٠°) وعند قيم مختلفة للانخفاض النسبي (h/b) وهي ٠,٢ ، ٠,٣ ، ٠,٤ . ويهتم الجزء الثاني من البحث بدراسة خصائص الجريان الأخرى ولذا أجريت مجموعة من التجارب لدراسة التغير في العوامل الأخرى المؤثرة على الجريان وتشمل الانخفاض النسبي (h/b) وكانت ٠,١ ، ٠,٢ ، ٠,٣ ، ٠,٤ ، ٠,٥ ، ٠,٦ وأخذت زاوية الميل للانخفاض عند المدخل والمخرج لقيم مختلفة وهي ١٥° ، ٣٠° ، ٤٥° ، ٦٠° ، ٧٥° ، ٩٠° ورقم فراود الابتدائي .وقد اشتقت معادلات تربط المتغيرات المختلفة للجريان ولايجاد الفقد النسبي للطاقة ورقم فراود الابتدائي. وتم اعداد منحنيات تطبيقية لابعدية توضح طبيعة وشكل التغير بين خصائص السريان المختلفة. وبتحليل النتائج العملية تبين أن نسبة الطاقة المبددة يزداد بزيادة الميل الطولي للمجرى وزاوية ميل الإنخفاض وكذلك بزيادة الانخفاض النسبي ورقم فراود. وقد تبين أن معدل الفقد النسبي في الطاقة المبددة يزداد بمعدل كبير وحتى زاوية ميل الانخفاض ٥٠° في الأمام والخلف وبعدها يقل معدل الزيادة في الطاقة المبددة إلى حد ما. وكذلك تم دراسة تأثير جميع المتغيرات المؤثرة على خصائص السريان وتم تحليلها ومناقشتها.

ABSTRACT

In this research paper, an experimental investigation was carried to study the turbulent structure and flow characteristics through inclined finite depression in sloping rectangular channel of constant width using Laser Doppler Anemometer (LDA). To study the turbulent structure , precise and accurate measurements of the mean and fluctuating flow quantities such as turbulence intensity components ($\acute{u}/U_o$ and v'/U_o) and mean velocity components ($\bar{u}/U_o$ and $\bar{v}/U_o$). The measurements were carried out along the flow depth at different cross-sections within and downstream of the finite depression. Also, the measurements were conducted at different relative height h/b and different finite depression angle θ in the longitudinal direction along the centerline and across the finite depression at different locations to assess the variation of the maximum turbulence intensities ($\acute{u}_{max}/U_o$ and v'_{max}/U_o). Experiments were conducted under different variables such as , bed slope , relative heights , relative length of finite depression to study the variation of the energy loss with the main parameters affecting the finite depression in sloping channel . The energy loss through the finite depression length was computed and correlated to the relevant parameters. These parameters include the bed slope , the upstream Froude number , the relative height ratio , the finite depression angle , the relative length ratio and the upstream head ratio . The effect of all these parameters on the energy loss through the finite depression were analyzed and discussed . Non – dimensional design curves were provided to relate the flow characteristics . The results show that , the turbulence intensities $\acute{u}_{max}/U_o$ and v'_{max}/U_o along the centerline beyond $x/h > 6.1$, $\acute{u}_{max}/U_o$ and v'_{max}/U_o were always higher in the case of 90° flow and lower for gradual 15° flow . This trend was exactly opposite as observed for $x/h < 3.2$, where the turbulence intensity was maximum for the 15° flow and minimum for the 90° flow , and the maximum of $\acute{u}_{max}/U_o$ and v'_{max}/U_o occurs in the intermediate zone $3.2 < x/h < 6.2$ for all cases. The finite depression angles

Accepted May 20, 2009.

$\theta < 15^{\circ}$ caused much lower turbulence data than that of angle $\theta = 90^{\circ}$ flow under the same conditions, whereas angles between 20° and 25° lead to higher turbulent velocities compared to a 90° flow. Also, beyond specific value of $\theta = 25^{\circ}$, turbulence intensities values were higher in the case of cross section x/h = 4 than that for cross section x/h = 1. The loss of energy increases by increasing the bottom slope, the relative height , the finite depression angle and upstream Froude number. The rate of variation of the energy loss was increased rapidly till the angle of finite depression was about 50°, such rate of increase was decreased about this value when the angle was 50° . The loss of energy was quite high at a relative height > 0.3.

1. INTRODUCTION :

The information regarding the turbulence characteristics in the transitionel structures is somewhat scanty. Paradoxically enough, the problem of separation of the main stream of flow at open channel transitions or at an abrupt change of the boundary attracted the attention of investigators since the earliest time and yet it remains one of the least understood and the most critical problems of fluid dynamics today. Open channel transitions have been studied extensively because of their use in water resources engineering and their efficacy in reducing the energy loss in hydraulic structures. Transitions are provided , whenever the size or the shape of the cross section of an open channel changes. Such changes are often required in natural and artificial channels for irrigation structures economically as well as for practical reasons. The transitions may be vertical or horizontal, contracting or expanding, sudden or gradually which are required for subcritical or supercritical flows. Thus the transition on the flow depends mainly of the boundary geometry, the discharge and the state of flow. The change in the cross section disturbs the flow in the contracted reach and near it from both upstream and downstream. The change in the channel cross section, slope, and / or alignment over a specified reach is termed local transition. Such channel transition is used mainly to avoid or minimize the excessive energy loss, to eliminate the cross waves, the resulting turbulence and to ensure safety of both the structure and the downstream channel reach. In the design of hydraulic structures, designers do their best to avoid sudden transition of the flow by sudden contractions to ensure smooth flow with minimum energy loss and to reduce turbulence pattern. The phenomenon is usually so complicated that the resulting flow pattern is not readily subjected to any analytical solution. So, a practical solution is possible, however, through experimental investigation. The present research deals only with vertical transitions through inclined finite depression. Studies on channel transitions and design of flume inlets include those of Attia [2], Nandana [14] and Vittal [19]. Formica [6] tested experimentally the various design for channel transition. The main results of Formica were reported in Chow [4]. The turbulent flow models in open channel flows were discussed by Grade [7], Rodi [16]; Nezu and Nakagawa [12]. Experimental investigation on turbulent structure of back facing step flow, have been reported by several investigators [1, 8, 13, 15]. Measurements of turbulence characteristics in open channel flows using LDA have been pointed by several investigators [3, 5, 9, 10, 11]. In the present investigation, the main objective is to study the turbulent structure and flow characteristics through inclined finite depression in sloping rectangular open channel and to asses the influence of relative height, bed slope, finite depression angle and relative length on the turbulence intensities ($\acute{u}/U_o$ and v'/U_o), mean velocity ratio components ($\bar{u}/U_o$ and $\bar{v}/U_o$) and the relative energy loss.

2.EXPERIMENTAL SETUP AND PROCEDURE :

The measurements were carried out in sloping glassed walls of 6mm thick rectangular open channel 7.0 m long, 10 cm width and 31 cm height . Fig 1 shows longitudinal section of the test flume . The water was supplied from a constant head tank to the flume at a desired discharge that is continuously monitored with an on-line orifice meter. A tail vertical gate was provided at the downstream end of the flume to maintain the required water depth of channel flow. The water was finally collected in a sump from where it was pumped back to the head tank by a pump. Depth measurements were carried using a needle point gauge with a reading accuracy of ± 0.1mm. Uniform flow conditions

were reached using a carefully designed inlet tank. The slope was adjusted using a screw jack located at the upstream end of the flume while at the downstream end, the flume was allowed to rotate freely about a hinged pivot. The slope was directly determined using a slope indicator. A downstream adjustable gate was used to regulate the tail water elevation. The finite depression with different angle of variations of 10°, 15°, 20°, 12°, 30°, 45°, 60°, 75° and 90° ; different lengths of 0.5, 1.0, 1.5, 2.0, 2.5 and 3.0 m; and different heights of 1, 2, 3, 4, 5 and 6 cm were fabricated from transparent prespex sheets. For each combination of finite depression angle, bed slope, relative height and relative length; five different flow rates ranging from 410 l/min to 302 l/min were used.

3. LDA MEASURING TECHNIQUE :

The experimental data were collected using two color back scatter LDA system. Figure 3 shows a block of the two component LDA set up used for the measurements. A five Watt Argon-ion Laser with two laser beams, one blue (488 nm) and one green (514.4 nm), were focused at a measuring point from one side of the channel through an optical lens. Two Burst Spectrum Analyzers (BSA) were used to evaluate the Doppler frequencies. Subsequent computer analysis consisted of velocity bias and outliner rejection. The number of samples taken at every point was 4000 bursts. This correspond to a simple averaging time of about 100 seconds. The data rate was about 40 – 50 per second. Before acquiring the data, the LDV signal was check for its quality on a Gold storage oscilloscope. The signal display as regular Doppler burst that correspond to a particle passing through the measuring volume. The measurements were taken at different locations, within and downstream of the finite depression for maximum discharge.

4.THEORETICAL APPROACH :

Figure 2 shows a definition sketch of flow through the finite depression in sloping rectangular cannel. The variables affecting the flow through the finite depression are shown on the figure and explained at the notation section. The functional relationship of the energy loss through the finite depression could be written as follows :

$$f_1(g , V_u , Y_u , Y_d , h , b_u , b_d , \Delta E , L , S_o , \theta) = 0 \quad \ldots\ldots\ldots(1)$$

Using the dimensional analysis, the following dimensionless relationship is obtained :

$$\frac{\Delta E}{Y_u} = f_2 \left[F_u , \frac{Y_d}{Y_u} , \frac{b}{Y_u} , \frac{L}{Y_u} , S_o , \theta\right] \ldots.(2)$$

It may appear better to analyze the energy loss through the finite depression as a ratio related to the upstream energy , E_u. Therefore, E_u was used instead of Y_u in the left hand side of equation (2) , which become :

$$\frac{\Delta E}{E_u} = f_3 \left[F_u , \frac{h}{b} , \frac{L}{b} , S_o , \theta\right] \ldots\ldots\ldots(3)$$

in which V is the velocity at the point of the flow depth Y with u for just upstream the finite depression and d just at the end of the finite depression.

From continuity equation

$$F_u^2 = (b_d / b_u)^2 \ (Y_d / Y_u)^3 \ F_d^2 \quad \ldots\ldots\ldots(4)$$

The above equation represents the relationship between F_u , F_d and Y_d / Y_u as parameters.

The energy loss is computed using the following expression:

$$Y_u + Q^2/2 g b_u^2 Y_u^2 = Y_d + Q^2/2 g b_d^2 Y_d^2 + \Delta E \quad \ldots\ldots\ldots(5)$$

Equation (5) may be rearranged to

$$Y_u + Y_u . F_u^2/2 = Y_d + Y_d . F_d^2/2 + \Delta E \quad \ldots\ldots(6)$$

Hence,

$$Yu (1+ F_u^2/2) = Yd (1+ F_d^2/2) + \Delta E \quad \ldots\ldots\ldots(7)$$

From equations (4) and (7), equation may be rearranged as:

$$F_u^2 = 2[(Y_d / Y_u - 1) + \Delta E / Y_u] / [1 - 1 / (b_d . Y_d / b_u . Y_u)^2] \quad \ldots\ldots\ldots(8)$$

The above equation represents the relationship between F_u , Y_d/Y_u and $\Delta E / Y_u$ as parameters

Again, Equation (5)could be written as follows:

$$\Delta E / E_u = Y_d / E_u [(1+ F_u^2/2) - Y_d / Y_u + F_u^2/2 (b_d / b_u)^2 (Y_d / Y_u)^2] \quad \ldots\ldots\ldots(9)$$

The above equation represents the relationship between the efficiency($E_d/E_u = 1-\Delta E/E_u$), $\Delta E/E_u$, Y_d/Y_u, F_u and (b_d/b_u) as dimensionless parameters

5. RESULTS AND DISCUSSION:

Fig . 4 (a) , (b) , (c) and (d) shows the variation of upstream Froude number F_u with (height to length ratio) h/L for different relative heights h /b = 0.1, 0.2, 0.3, 0.4, 0.5 and 0.6 for bed slopes S_o = 0.0, 0.010, 0.015 and 0.025 respectively at a fixed finite depression angle θ = 15°.The resulting curves indicate that for the same value of S_o and h/b of finite depression , both F_u and h/L increased with the decrease of the value of relative length L/b . Also for the same h/L , F_u increased and both h/b and L/b decreased with the range 0.001 < h/L< 0.120. Fig .5 (a) , (b) , (c) and (d) depicts the variation of upstream Froude number F_u with h/L for different relative lengths L/b = 5 , 10 , 15 , 20 , 25 and 30 for bed slopes S_o = 0.0 , 0.010 , 0.015 and 0.025 respectively at a fixed finite depression angle of θ = 15° . For each S_o , the study of each plot demonstrate that with the increase of h/L , F_u decrease and h/b increases for the same L/b. At the same value of F_u , h/L increased with the decreasing value of L/b . Also , F_u increases with increasing value of bed slope S_o.

The variation of the relative energy loss $\Delta E/E_u$ with finite depression angle θ for different relative heights h/b = 0.1 , 0.2 , 0.3 , 0.4 , 0.5 and 0.6 are presented in Fig.6 (a) , (b) , (c) and (d) for different values bed slope S_o = 0.0, 0.010, 0.015 and 0.025 respectively . From figure, it could be observed that , the trend is almost the same for all other relative heights h/b . Also , for a fixed S_o , the trend of variation between $\Delta E/E_u$ and θ is increasing with a nonlinear trend . At a particular θ, $\Delta E/E_u$ increases as the relative height increases. As the angle of inclined finite depression θ increases up to 50°. The rate of increase in the $\Delta E/E_u$ is relatively high for all values of h/b , being very high for the h/b of 0.5 and 0.6. Above θ=50°, the increase in the energy loss is much slower. The energy loss is the least value for h/b of 0.1 and a maximum value of h/b of 0.6. It is relatively small up to the relative height of 0.3. This figure indicate that the slope has a remarkable effect on the energy loss, with increasing bed slope the energy loss is increased. Figure 7 (a) ,(b) , (c) and (d) presents the variation of energy loss $\Delta E/E_u$ with bed slope S_o for different relative heights h/b of 0.1 , 0.2 , 0.3 , 0.4 , 0.5 and 0.6 at different finite depression angle θ = 15° , 30° , 45° and 90° respectively. From figure, it could be observed that for a fixed θ, the variation between $\Delta E/E_u$ and S_o is increasing with nonlinear trend. Also, at a particular S_o , $\Delta E/E_u$ increases as the relative height h/b increases. This figure indicates that the finite depression angle θ has a remarkable effect on the energy loss, with increasing the angle of finite depression θ the energy loss is increased. Figure 8 (a), (b), (c) and (d) depicts the variation of upstream Froude number F_u with relative energy loss $\Delta E/E_u$ for different relative heights h/b of 0.1 , 0.2 , 0.3 , 0.4 , 0.5 and 0.6 for different bed slopes S_o of 0.0 , 0.010 , 0.015 and 0.025 respectively at a fixed finite depression angle θ = 90°. The relationship between F_u and $\Delta E/E_u$ is a family of curves which are similar hyperbolas of a higher order according to Equation (5). It can be shown that, from this figure, with the same value of bed slope, the value of $\Delta E/E_u$ increases with the increasing value of F_u. Also, with the same value of F_u, the value of $\Delta E/E_u$ increases with the increasing value of h/b. Also, it is observed that an extension of the lower sides of the curves through the point (F_u = 0, $\Delta E/E_u$ = 0) gives the hydrostatic case.

Measurements were made for various flow conditions. However, only representative results are presented here. The turbulence intensity components and velocity components are non-dimensionalized by the streamwise free stream velocity in x-direction U_o. The water depth is non- dimensionalized by the streamwise free stream water depth y_o. Turbulence at the wall was construed to be turbulence at a very location from the wall of the order of 3mm as observed in LDA experimentation, and not at the wall itself perse. At the boundary velocity and turbulence are zero. Figure 9 shows the streamwise mean velocity profiles $\bar{u}/U_o$ in the finite depression with angle of variation θ of 15° and 30° at different positions. The streamwise mean velocity $\bar{u}/U_o$ varies considerably according to the finite depression angle θ and the flow conditions. The flow acceleration is seen to be maximum in case of the 30° gradual finite depression. Interestingly , the 15° gradual finite depression not only reduce the flow acceleration with their gradients , but also influence the viscous effects close to the channel bed since wall shear stress deduced from the

velocity of the very first point from the surface , seems to vary with the geometry. The wall shear stress of the finite depression first increases when gradient is made $\theta = 30^o$ and then it decreases when the gradient is further changed to $\theta = 15^o$. Such reduction in the wall shear stress is a desired result and would be expected to reduce the energy loss. It can be seen that with decreasing finite depression inclination, the maximum negative (counter streamwise) velocities in the recirculation zone are reduced. In the external flow over the separation bubble, the maximum positive velocities are reduced as well for flattened depression. For flatter finite depressions, the maximum mean velocity u^+_{max} moves toward the middle of the channel behind the finite depression edge. With increasing angle θ the velocity profiles become more and more asymmetric and the velocity gradient (du/dy) in the shear layer is growing. Near the corner location of the finite depression, reversal flow could be observed for $\theta = 30^o$ as shown in Fig 9 at x/h of 1 , 2 , 3 and 4 , as could be seen by the sharp of the velocity profile , and as was observed by dye injection. In Figure 12 , the velocity distributions in a channel cross section are plotted exemplarily for four different finite depression angles $\theta = 10^o$, 15^o , 20^o and 25^o at channel position x/h = 4 for the bed slope S_o = 0.0. The described changes in the velocity data with decreasing finite depression angle θ could be seen. Smaller positive mean velocities in the external flow and the smaller negative velocities in the recirculation zone reduce the dimensions of the separation bubble for flattened finite depression angles. The maximum negative velocity $\bar{u}_{max}/U_o$, is shown in Fig. 13 for different finite depression angle variations θ of 15^o , 20^o , 25^o , 30^o and 90^o. The maximum of $\bar{u}_{max}/U_o$ is registered for all finite depression inclinations always in the middle of the separation zone. For $\theta = 25^o$ and $\theta = 30^o$ the peak of the maximum counter streamwise velocities is up to 9% higher than of the 90^o finite depression flow. Also , it could be seen that steeper inclination angles result in higher maximum negative (counter streamwise) velocities $\bar{u}_{max}/U_o$ in the recirculation regime and the rotating mass flux of the total throughout is growing in the rang between 20^o and 30^o. Corresponding to the velocity profiles (Fig .9) , measurements of vertical mean velocity $\bar{v}/U_o$ were conducted for gradual finite depression of $\theta = 30^o$ at the same flow conditions and locations at which the streamwise mean velocities were measured. Fig .11 presents the profile of vertical mean velocity distribution $\bar{v}/U_o$ at various locations. The profile of $\bar{v}/U_o$ assumes both positive and negative values at the same section and hence the zero value at some intermediate locations. This nature of variation, viz., change from positive to negative magnitude and vice versa occured almost at all the sections. The zero magnitude of vertical velocity component $\bar{v}/U_o$, occurs at more than one point at several locations. The magnitude of $\bar{v}/U_o$ increases steadily from the entrance section, the magnitude gradually decreases reaching small value at the farthest downstream of x/h = 25. At exact entrance location, velocity $\bar{v}/U_o$ was negative all along the vertical height. This observations may be attributed to the expanding velocity field and diversion of flow at the finite depression corner. The observation of the multiplicity of null point to the three dimensional interaction between the entrance flow to the finite depression almost with negative vertical velocity component. The influence of depression itself along with the bed impeding the downward component of velocity . This complex interaction would influence the flow pattern giving rise to multiplicity null point.

Root mean square (RMS) values of streamwise component of turbulence intensity (u`) carried out nondimensional with respect to the streamwise mean free stream velocity $U_o$. Fig.10 shows turbulence intensity profiles $u`/U_o$ as a function of dimensionless channel depth y/y_o of the gradual finite depression for $\theta = 15^o$ and 30^o at different locations which are measure of fluctuations about the respective mean velocity shown in Fig.9. The conditions of the flow at the inlet of the finite depression cause unidirectional distortion of the fluid elements which may be expected to produce nonhomogeneous and anisotropic turbulence. Under the action of dynamic process, the turbulence was produced to some degree all over the field. The streamwise turbulence intensity $\acute{u}/U_o$ grows rapidly after the flow separation and is spreading in the y-direction further downstream. An increase of the inclination angle from 15^o to 30^o does increase

enormiously the turbulence intensities after the finite depression edge. In the wall region defined by y/y_o <0.2 the turbulence intensities $\acute{u}/U_o$ have substantially small magnitude closer to the wall. With the increasing distance from the boundary, the turbulence intensities increases in wall region tending towards a maximum in the intermediate region (core region) defind by $0.2 < y/y_o < 0.6$, where is the location of the maximum value of the turbulence , reaching a lower value in the free surface region defined by $y/y_o > 0.6$ subsequently. It has been observed during this experimentation, that surface waves play an important role in the turbulent production.As a comprehensive observation, it was noted that, the streamwise turbulence $\acute{u}/U_o$ for 30° – finite depression flow was always greater than that for $\acute{u}/U_o$-15° finite depression flow. The slight increase of the turbulence intensity in the shear layer and the small turbulent growth in the y-direction for these flat finite depression angles did not influence strongly the turbulent of the flow in the upper channel section. x/h > 25 the maximum turbulence intensity was reduced almost to the same level of the streamwise free stream turbulence intensity. In Fig. 14 normalized turbulent velocity profiles are shown exemplarity for different finite depression inclinations at x/h = 4. It could be seen that finite depression angle variations θ < 15° result in much lower turbulence data than a 90° – finite depression flow under same conditions, where as finite depression angles 20°< θ < 25° lead to higher turbulent velocities compared with the 90°- finite depression. This is a particular case for finite depression angles 20° < θ < 25° in which the influence of near wall of the finite depression inclination on the flow field becomes a maximum. It could be shown that for a finite depression angle of 20° - 25°, a maximum value occurs in the cross section under investigation as might be seen in Figure 15. It could be proved that in this particular range of angle, turbulent intensity becomes maximum and the turbulent data exceed the values of the 90° finite depression flow. Fig.15 depicts the variations of maximum streamwise turbulence intensities $u`_{max}/U_o$ in cross section as a function of depression angle at different positions of the finite depression. Turbulence $u`_{max}/U_o$ rises rapidly to reach maxima with subsequent monotonous decrease with increasing the depression angle. Generally, the maximum turbulence intensities occur almost at the range of depression angles of (20°-30°) at the different locations. Clearly, the trend of maximum streamwise turbulence intensities $u`_{max}/U_o$ variation were quite similar in all different locations. It may be concluded that, beyond specific value of θ = 25° , $u`_{max}/U_o$ values were always higher in case of cross section x/h = 4 and lower for cross-section x/h = 1. Figures 16 and 17 show the variation of turbulence fluctuations in the maximum streamwise and transverse direction (u_{max}/U_o) and ($v`_{max}/U_o$) along the centerline at different gradual finite depression of θ = 15° , 45° and 90° for bed slope $S_o$ = 0.0 at h/b = 0.5 .Clearly, the trend of ($u`_{max}/U_o$ and $v`_{max}/U_o$) variation were similar in all the cases of finite depression under study . Turbulence rises rapidly to reach maxima with subsequent monotonous decrease along the distance away from entrance of the finite depression. The maximum values of the streamwise turbulence intensities ($u`_{max}/U_o$) were observed to be 22% , 20% and 17.5% at x/h of 5, 6 and 5 for gradual finite depression of θ = 45° , 90° and 15° respectively. The maximum values of the transverse turbulence intensities ($v`_{max}/U_o$) were observed to be 17% , 15.5% and 14.5% and occur at x/h of 5,5.5 and 3.5 respectively. Thus it may be thus concluded that the turbulence intensity beyond x/h > 6.1 from the entrance edge of the finite depression decreases with the angle of inclination decreases. The trend is reverse for x/h < 3.1 where the turbulence was intensity was maximum for gradual finite depression of θ = 15° and minimum for the 90° finite depression flow. At x/h equals 3.1, the values of turbulence intensities are same for both gradual finite depression of θ = 15° and 45°. In the intermediate zone 3.1 < x/h < 6.1, the turbulence was maximum for all the cases of gradual finite depression. From the general trend of variation of both the turbulence intensities $u`/U_o$ and $v`/U_o$ at may be concluded that the turbulence intensities decrease from x/h = 3.2 in the upstream and beyond x/h = 5 in the downstream sections in all finite depressions. This decrease began earlir for gradual finite depression θ = 15° at x/h = 3.2 and later at x/h = 5 for sudden finite depression of θ = 90°. Before these locations in all the cases both the turbulence intensities $u`_{max}/U_o$ and $v`_{max}/U_o$ were higher for gradual finite depression θ = 15° at a

typical location of x/h = 2. This was due to sudden curvature imparted to streamline flow along the finite depression wall at the upstream end. Some separation was observed at the edge, which might have caused this increase in the case of sudden finite depression. Again, it may be concluded that downstream the finite depression beyond specific values of x/h for instance 6.1 as stated above, turbulence intensities $u`_{max}/U_o$ and $v`_{max}/U_o$ are always higher in the case of sudden finite depression $\theta = 90^o$ and lower for most gradual finite depression $\theta = 15^o$. This trend is exactly opposite as observed for x/h < 3.2. Figs.18 and 19 present the variation of maximum streamwise and vertical turbulence intensities $u`_{max}/U_o$ and $v`_{max}/U_o$ along the centerline at different relative height h/b of 0.2 , 0.3 and 0.4 for bed slope So = 0.0 at finite depression angle $\theta = 15^o$. The trend $u`_{max}/U_o$ and $v`_{max}/U_o$ variation are similar in the two cases of finite depression. The turbulence rises rapidly beyond x/h > 1.5 attaining maximum value between the reach defined by 3 < x/h < 5 in the finite depressions. For the region beyond x/h = 5, turbulence decreases continuously at slower rate for finite depressions. Generally, maximum streamwise and vertical turbulence intensities occur at the same location with slight noticed for relative height h/b of 0.4. The maximum values of the streamwise turbulence intensities $u`_{max}/U_o$ were observed to be 17.5% , 15.1% and 11.9% occurring at x/h of 4.3 , 4.2 and 4.1 for relative height h/b of 0.4 , 0.3 and 0.2, respectively. The vertical turbulence intensities $v`_{max}/U_o$ with the maximum values 14% , 11% and 9.5% occur at x/h 2.9 , 2.8 and 2.7 of the relative heigh h/b of 0.4 , 0.3 and 0.2 respectively. It may be concluded from the general trend of variation of both the turbulence intensities u_{max}/U_o and v_{max}/U_o that the turbulence intensities decrease from x/h = 4 in the upstream direction.

6. CONCLUSIONS:

An experimental investigation is conducted on the flow structure through inclined finite depression in sloping open channel. The following conclusions may be stated.

(A) The energy loss $\Delta E/E_u$ increases by increasing the bottom slope S_o and the relative height h/b with more increase in the energy dissipation. At a fixed bed slope, the loss of energy increases by increasing the upstream Froude number F_u and the relative height at a constant finite depression angle θ. At the same values of S_o and h/b, both F_u and h/L increase with the decrease of the value of relative length L/b. Also for the same value of h/L, F_u increase and both h/b and L/b decrease. Also, it could be concluded that the variation of the energy loss with range of θ, it appears that The loss of energy increases rapidly up to $\theta = 50^o$. But above this angle ($\theta = 50^o$) the effect of the boundary is insignificant and with decreasing θ, the energy loss decreases. The energy loss is quite high if the relative height h/b > 0.4. Thus, $\theta=50^o$ appears to be critical defining a border value between the maximum loss of energy and the value up to which energy loss increases rapidly as θ increases from 0^o to 50^o. The results indicate that, the most significant in loss of energy occur with finite depression angle in the range less than 50^o.

The maximum negative (counter streamwise) velocity $\bar{u}_{max}$ is registered for all finite depression inclinations always in the middle of the separation zone. The magnitude of vertical mean velocity $\bar{v}/U_o$ increases steadly from the entrance section, the magnitude gradually decreases reaching small value again at the farthest downstream. The profile of $\bar{v}/U_o$ assumes both positive and negative values at the same section and hence the zero value at some intermediate locations.

(B) The turbulence intensities $u`_{max}/U_o$ and $v`_{max}/U_o$ along the centerline beyond x/h > 6.1, $u`_{max}/U_o$ and $v`_{max}/U_o$ are always higher in the case of 90^o flow and lower for gradual 15^o flow, this trend is exactly opposite as observed for x/h < 3.2 where the turbulence intensity is maximum for the 15^o flow and minimum for the 90^o flow, and the maximum of $u`_{max}/U_o$ and $v`_{max}/U_o$ occurs in the intermediate zone 3.2 < x/h < 6.1 for all the cases.

The turbulence intensities $u`_{max}/U_o$ and $v`_{max}/U_o$ along the flow depth were lower at the bed in the wall region defined by $y/y_o < 0.2$ and the free surface region defined by $y/y_o \geq 0.2$ and the minimum values of $u`/U_o$ and $v`/U_o$ occur at the same location of the profiles, either close to the bed or close to the free surface. The maxima of u`

$/U_o$ and v'/U_o being located approximately at the same location of the profiles in the intermediate core region defined by $0.2 < y/y_o < 0.6$. The u'/U_o and v'/U_o increase with increasing relative height h/b, at which the profiles of u'/U_o and v'/U_o become smoother and more uniform. As a comprehensive observation, it was noted that, u'/U_o was always greater compared to the v'/U_o, where the trend of variation being similar. After 25 finite depression heights (x/h>25) the maximum turbulence intensity was reduced almost to the same level of the streamwise free stream turbulence intensity. It can be concluded that, finite depression angles $\theta \leq 15°$ result in much lower turbulence data that $\theta = 90°$ flow under same conditions, whereas $20° < \theta < 25°$ lead to higher turbulent velocities compared with a $\theta = 90°$ flow. This case for $20° < \theta < 25°$ where the influence near the wall of the finite depression inclination on the flow field became a maximum at different locations .Also, it may concluded that, beyond specific value of $\theta = 25°$, turbulence intensities values are higher in the case of cross section x/h = 4 and the lower for cross section x/h = 1.0.

7. NOMENCLATURE:

b : Channel width
b_u : Upstream channel width .
b_d : Downstream channel width .
$\bar{u}$: Streamwise mean velocity component in x-direction.
$\acute{u}$: Streamwise component of turbulence intensity in x- direction (RMS).
u_o : Streamwise mean free stream velocity (averaged over the cross section).
h : Finite depression height.
L : Finite depression length.
Y_u : Upstream water depth .
Y_d : Downstream water depth .
F_u : Upstream Froude number .
F_d : Downstream Froude number .
E_u : Upstream specific energy .
E_d : Downstream specific energy .
ΔE : Energy loss .
Q : Discharge .
S_o : Bed slope .
g : Acceleration due to gravity .
θ : Finite depression angle.
$\bar{v}$: Vertical mean velocity component in y - direction.
v' : Vertical fluctuating velocity component in y-direction (RMS).
x : Longitudinal axis along channel length.
y : Transverse axis along channel height.
y_o : Free stream water depth.
rms : Root mean square.

8. REFERENCES:

1- Antoniou, J., and Bergeles, G., (1998), "Development of the Reathachment Flow Behind Surface Mounted Two – Dimensional Prisms", ASME J. of.Fluids Engg., Vol. 110, pp. 127 – 133.

2- Attia, M.I. and Josh, S.G., (1995)"Experimental Studies of Turbulent Flows in Sudden and Gradual Open Channel Transitions Using Laser Doppler Velocimetry" Proc. Of 22nd National Conf. on Fluid Mech. and Fluid Power (FMFP), Editors, V. Ganesan, Indion Institute of Tech., Madras, India, Madras, pp. 139 – 147 , 13 – 15 December.

3- Amino, R.S., and Goel, P., (1985) "Computations of Turbulent Flow Beyond Backward Facing Steps Using Reynolds Stress Closure", AIAA J., Vol. 23, No. 23, No. 9, pp. 1356 – 1361.

4- Chow, V.T., (1959) "Open Channel Hydraulics", Mc Graw Hill Book Co., New York, pp. 461 – 468.

5- Etheridge, D.W., and Kemp, P.H., (1978), "Measurements of Turbulent Flow Downstream of a Rearward Facing Step", Fluid Mech. No.3

6- Formica, G., (1955), "Preliminary Tests on Head Losses in Channels due to Cross Sectional Changes," L'Energia Electrical, Milano, Vol. 32, No. 7 , pp. 554 – 568, July (in French).

7- Grade, H. , (1993), "The Turbulent Flow Models in Open Channel Flows" Monograp, A.S. Balkema Puplishers, New Road, V.T 08079, New Dehi, India.

8- Nezu, I., and Nakagawa, (1995), "Experimental Investigation on Turbulent Structure of Backward Facing Step Flow in an Open Channel", J. of Hydr. Research, Vol. 25, No. 1

9- Kironoto, B.A., and Grad, W.H., (1994), "Turbulence Chareacteristics in Rough Open Channel Flow", Proc. Inst. Civ. Eng. Water, Maritime Energ., 98.

10- Melelland, S., Ashworth, p., Best, J., and Livesey, J., (1999), " Turbulence and Secondary Flow over Sediment Strips in Weakly Bimodal Bed Material," J. Secondar Flows, 125 (5), 463-473.

11- Nezu, I., and Rodi, W., (1986), "Open Channel Flow Measurements with a Laser Doppler Velocimetry," J. Hydraulic Eng. ASCE, 112, pp.335-355

12- Nezu, I., and Nakagawa, H., (1983), " Turbulence in Open Channel Flow," IAHA-Monograph, A.A.Balkma Publishers, Old Post Road, Brookfield, VT05036, USA.

13- Nakagawa, H., and Nezu, I., (1987), "Experimental Investigation on Turbulent Structure of Back Facing Step Flow in an Open Channel", J. Hydraulic Research, IAHR, 25, pp. 67-88.

14- Nandana Vittal, (1978), "Direct Soluations to Problems of Open Channel Transitions", Proc. Of the ASCE, Vol-104, No.HY11.

15- Ruck, B. and Makiola, B., (1990), "Flow over a Single Sided Backward Facing step with Step Angle Varition", Proc. 3rd Int. Conf. of Laser Anemometry, BHRA, Sptinger-Verlag, UK, pp. 369-378.

16- Rodi, W., (1993), " Turbulence Models and their Application in Hydraulics," IAHR Monograph, A.A. Balkema Publishers, Old Post Roadfield, VT 05036, U.S.A.

17- Song, T., and Chinew, Y., (2001)," Turbulence Measurement in Nonuniform Open Channel Flow Using Acoustic Doppler Velocimeter (ADV)," J. Eng. Mech., 127 (3), 219-231.

18- Sukhodolov, A., Thiele, M., and Bungartz, H., (1998), "Turbulence Structure in a River Reach with Sand Beds," Water Resour. Res., 34 (5), 1317-1334.

19- Vittal, N., and Chirangeevi, V.V., (1983), "Open Channel Transitions : Rational Methods of Design," J. of Hyd. Div., ASCE, Vol. 109, No. 1, pp. 99-115.

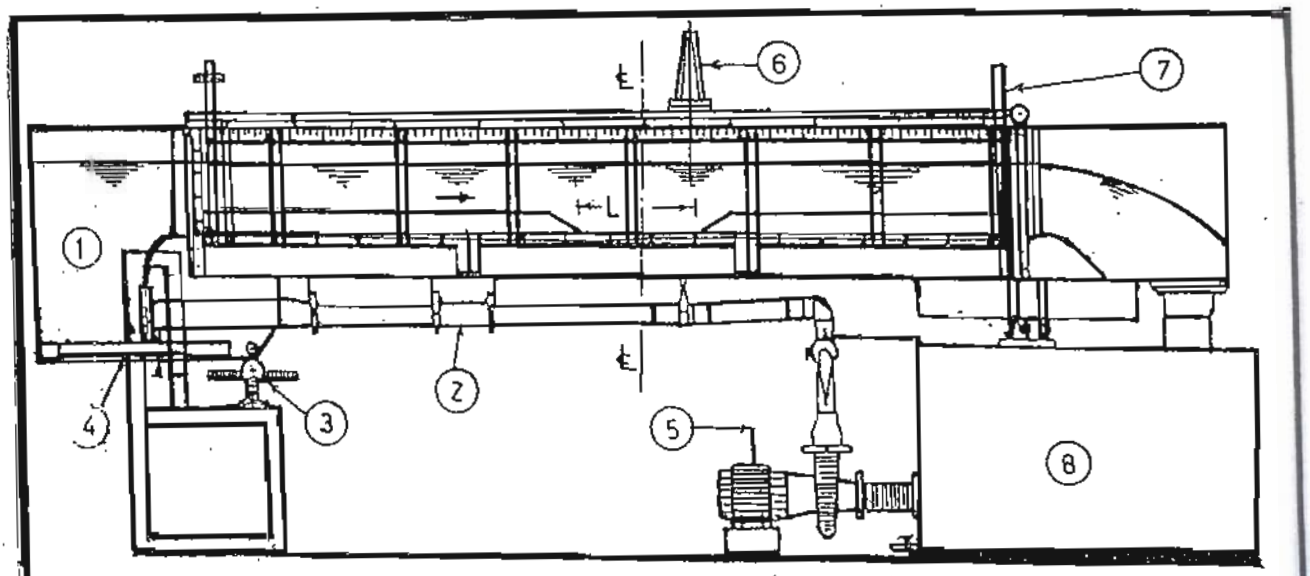

Fig. 1 Schematic sketch of test facility

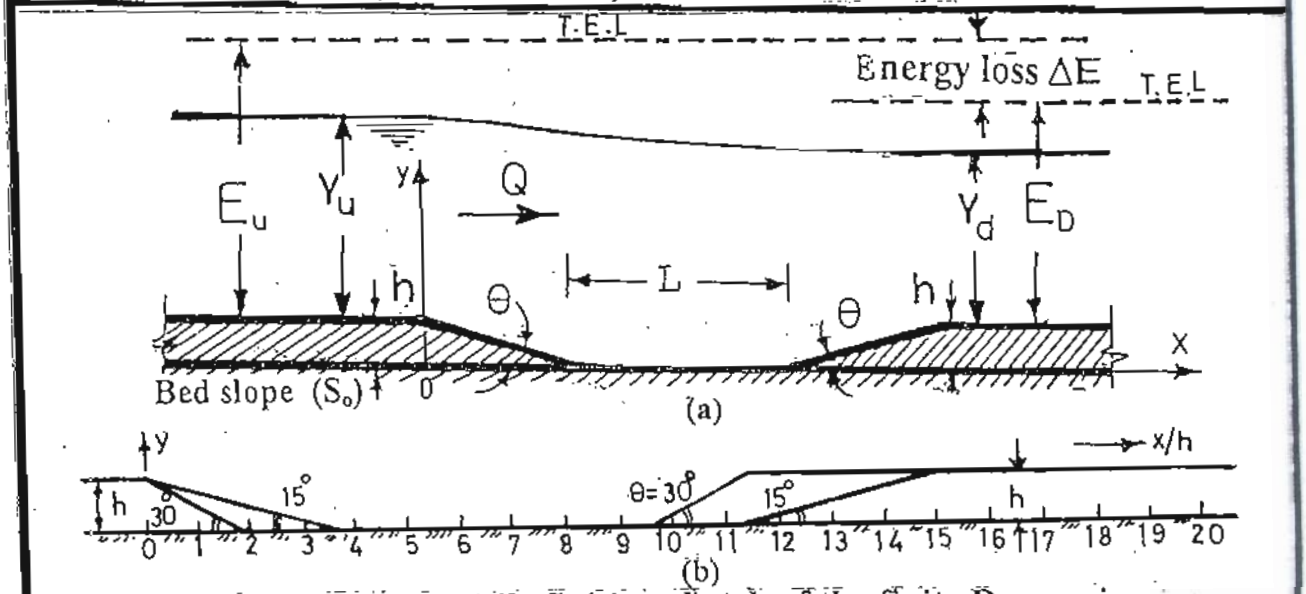

Fig. 2 (a)and(b) Definition sketch of the finite Depression

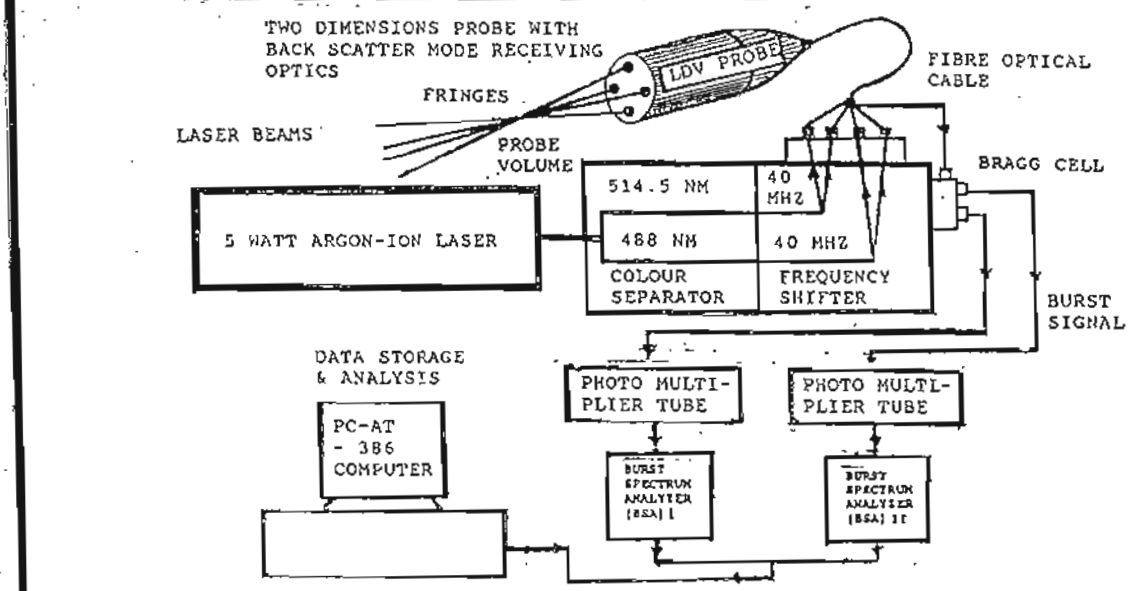

Fig. 3 Block diagram of the laser Doppler Velocimetry

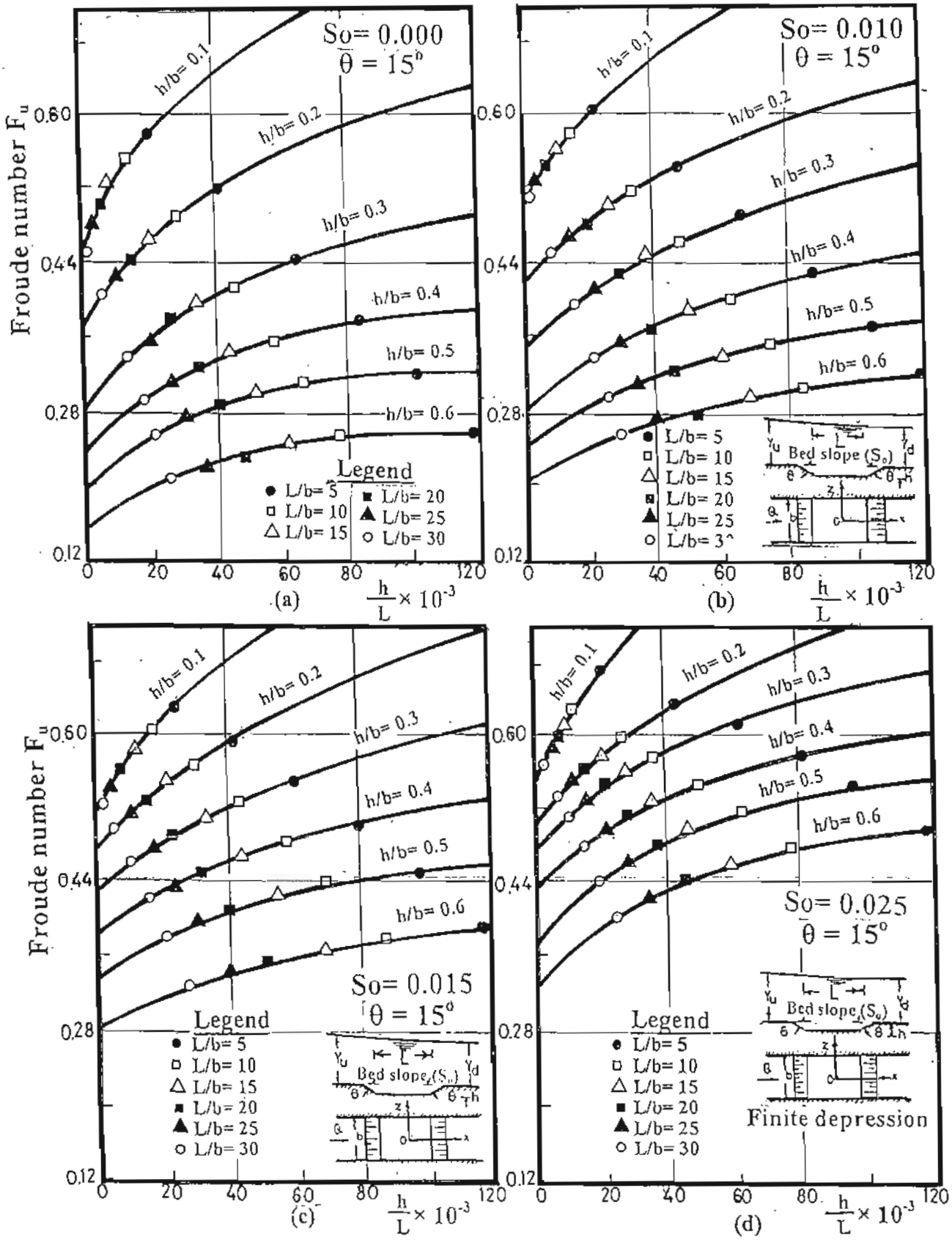

Fig. 4 (a),(b),(c)&(d) Variation of upstream Froude number F_u with h/L for different values of h/b at θ = 15° for different values of So

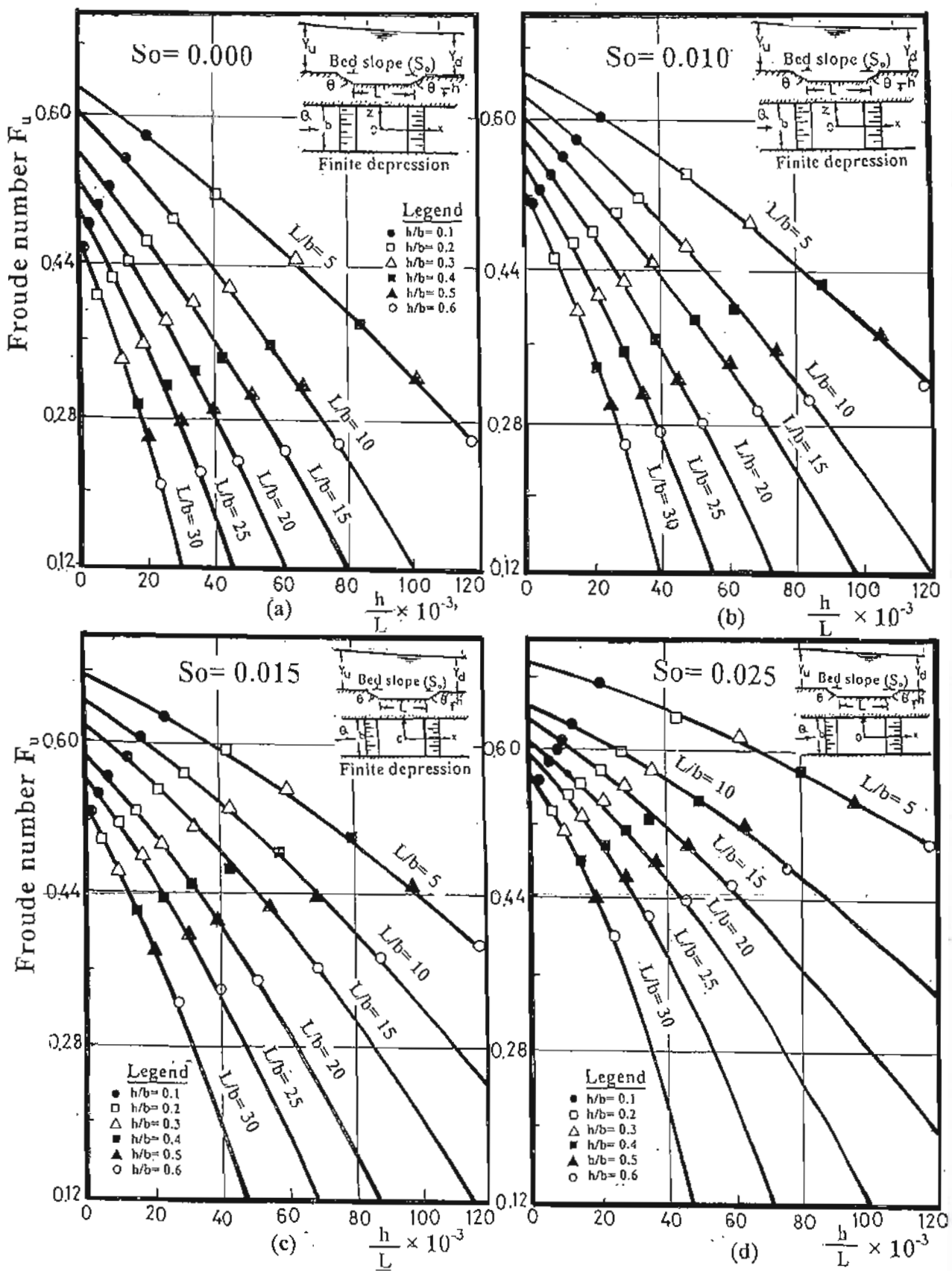

Fig. 5 (a),(b),(c)&(d)Variation of upstream Froude number F_u with h/L for different values of So at $\theta = 15^{\circ}$

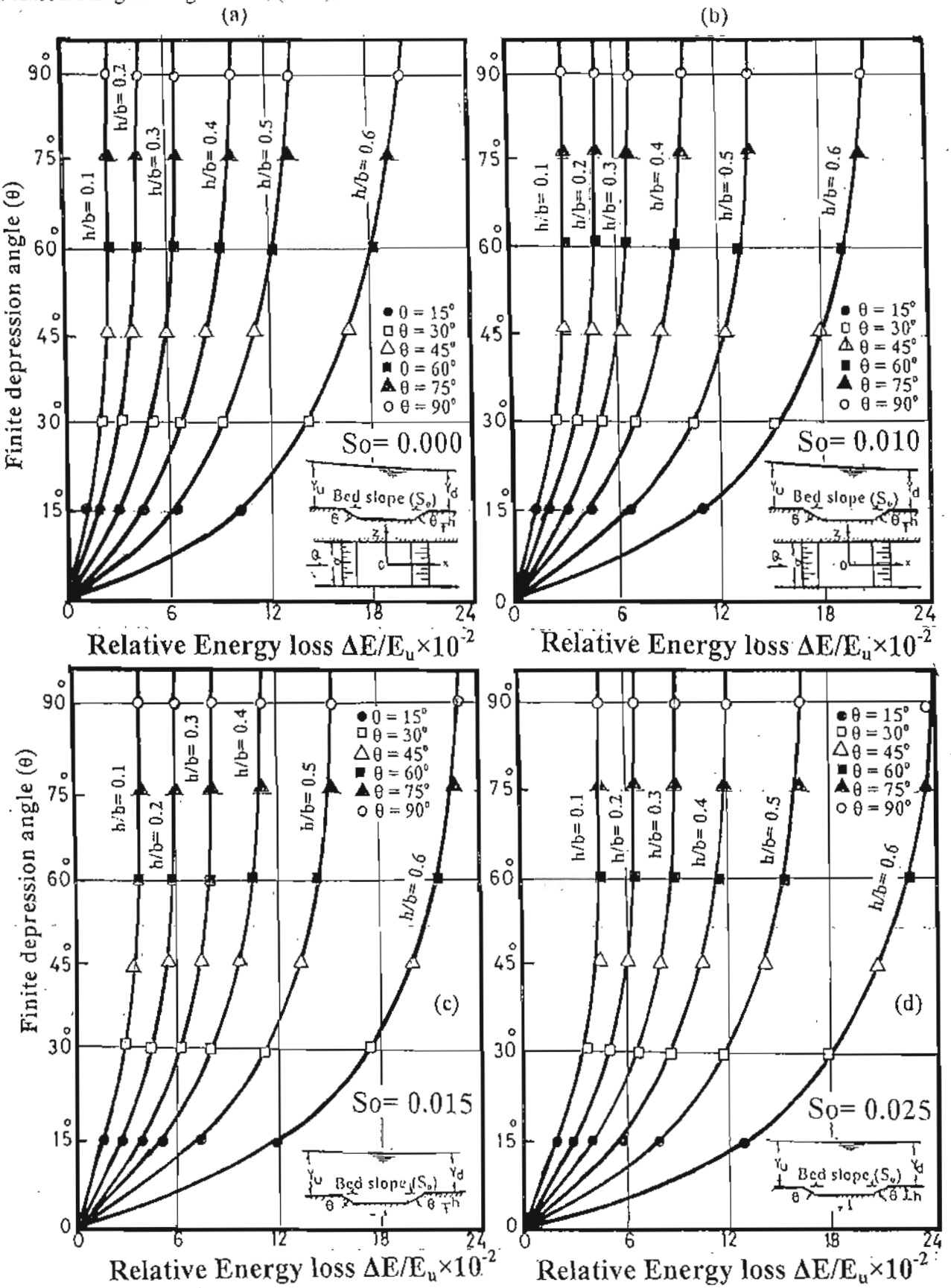

Fig. 6 (a),(b),(c)&(d)Variation of relative energy loss $\Delta E/E_u$ with finite depression angle θ for different values of relative height h/b at different values of bed slope S_o

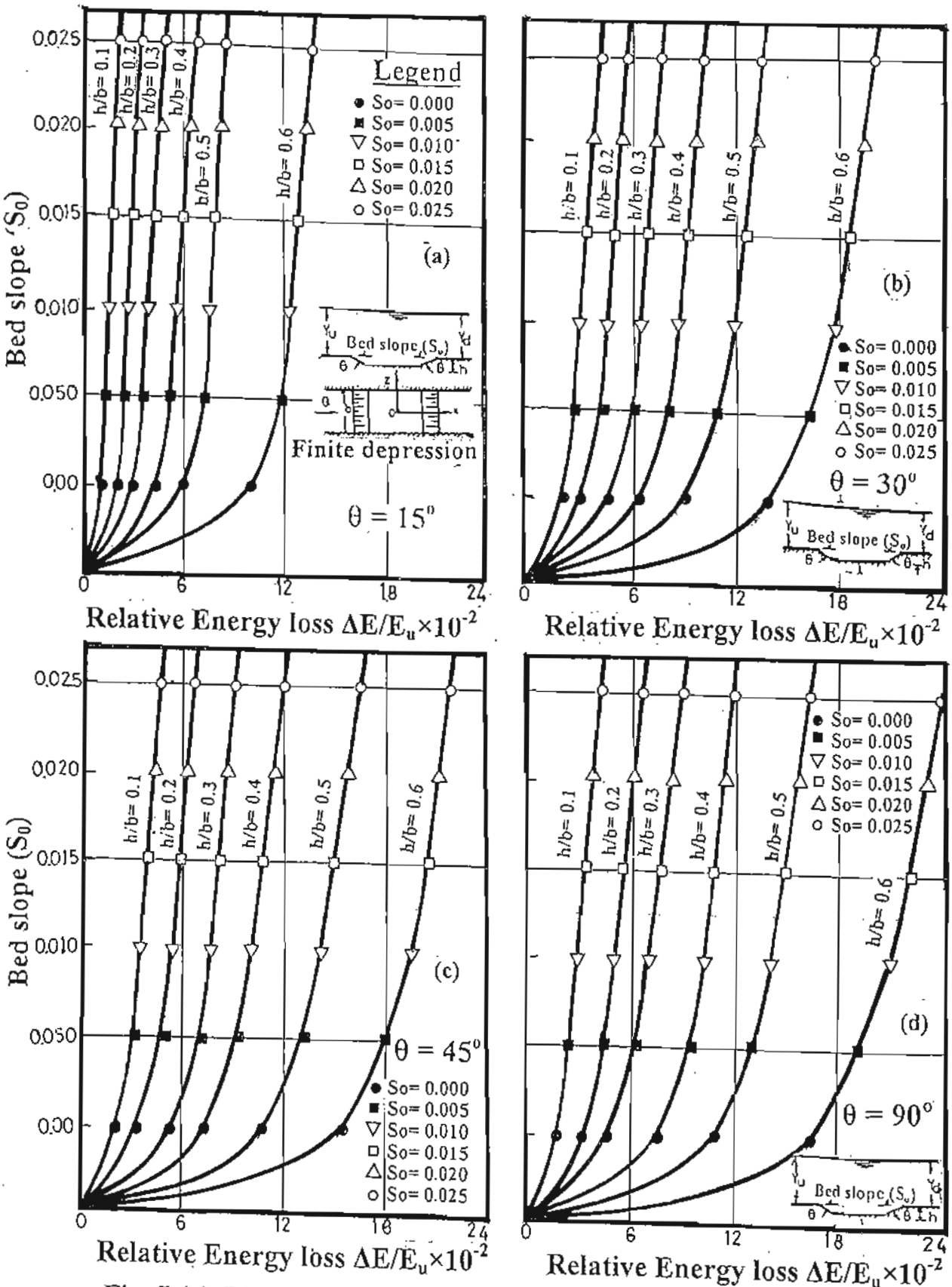

Fig. 7 (a),(b),(c)&(d)Variation of relative energy loss $\Delta E/E_u$ with bed slope S_o for different values of relative height h/b at different values of angle θ

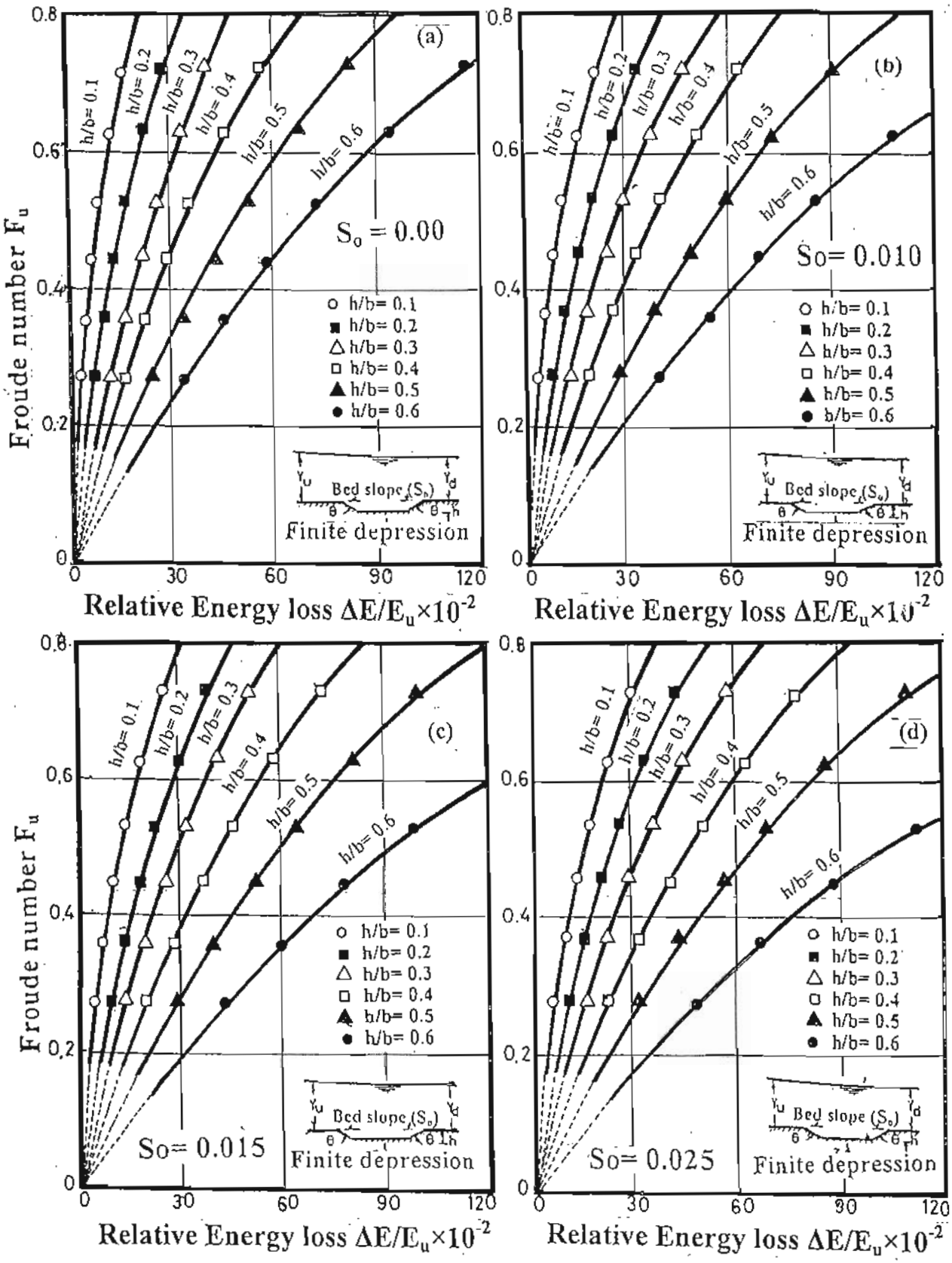

Fig. 8 (a),(b),(c)&(d) Variation of upstream Froude number F_u with relative energy loss $\Delta E/E_u$ for different values of h/b at different values of So

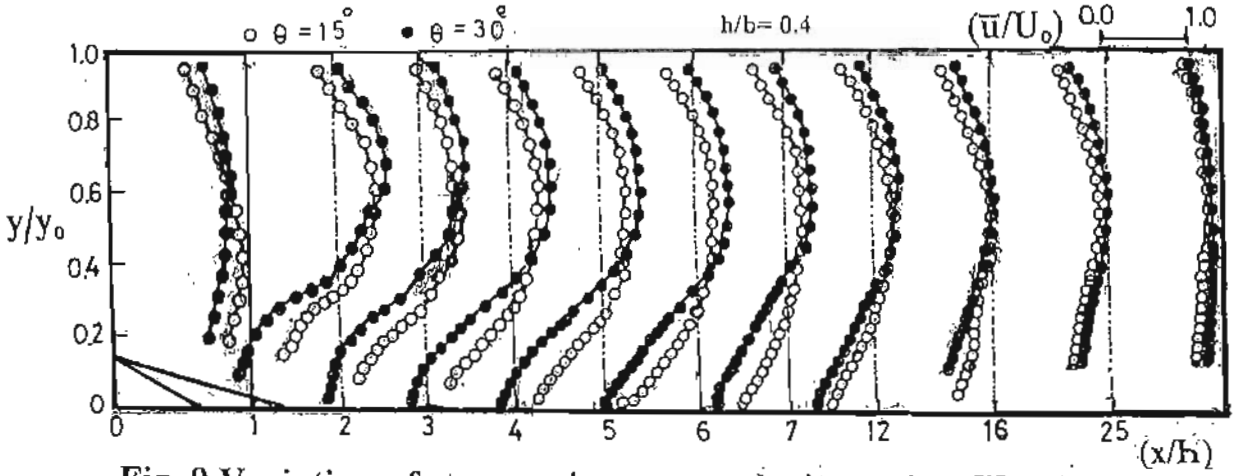

Fig. 9 Variation of streamwise mean velocity ratio $\bar{u}/U_o$ with y/y_o at different positions for $\theta=15^\circ$ and 30° and $S_o= 0.0$

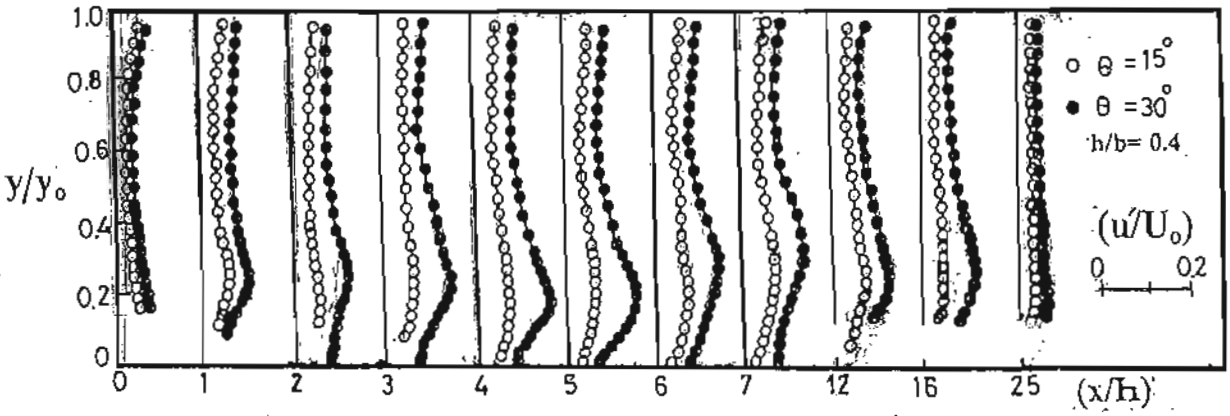

Fig. 10 Variation of streamwise turbulence intensities $\acute{u}/U_o$ with y/y_o at different positions for $\theta=15^\circ$ and 30° and $S_o= 0.0$

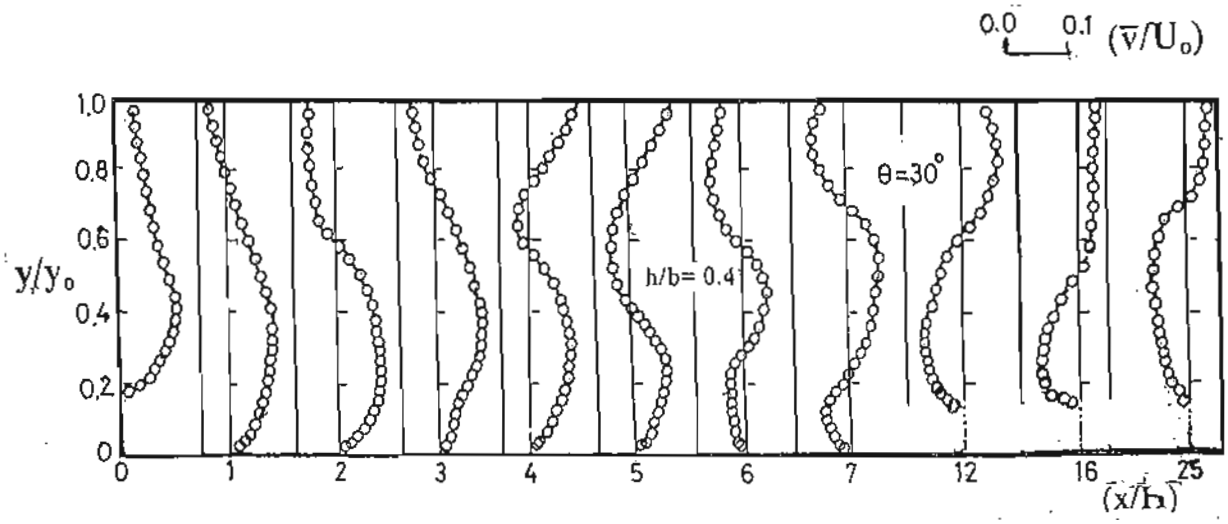

Fig. 11 Variation of vertical mean velocity ratio v/U_o with y/y_o at different positions for 30°

Mansoura Engineering Journal, (MEJ), Vol. 34, No. 2, June 2009.

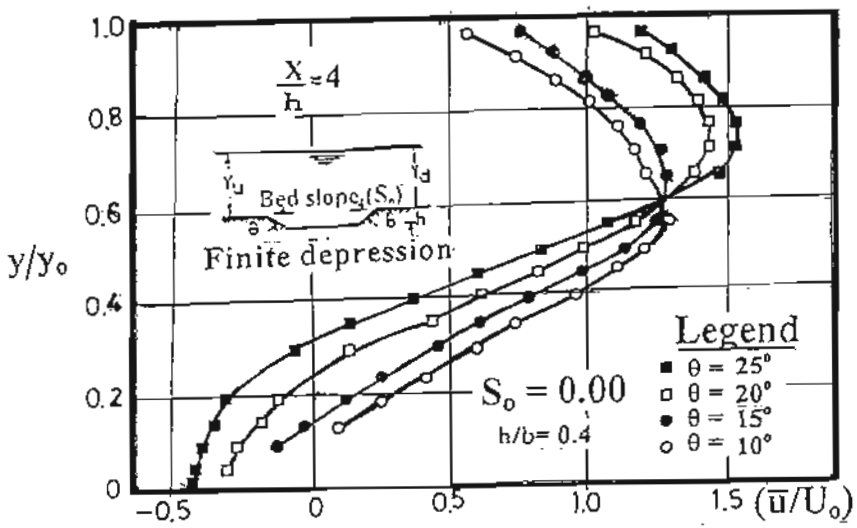

Fig. 12 Variation of streamwise mean velocity ratio $\bar{u}/U_o$ with y/y_o For different angles at x/h = 4

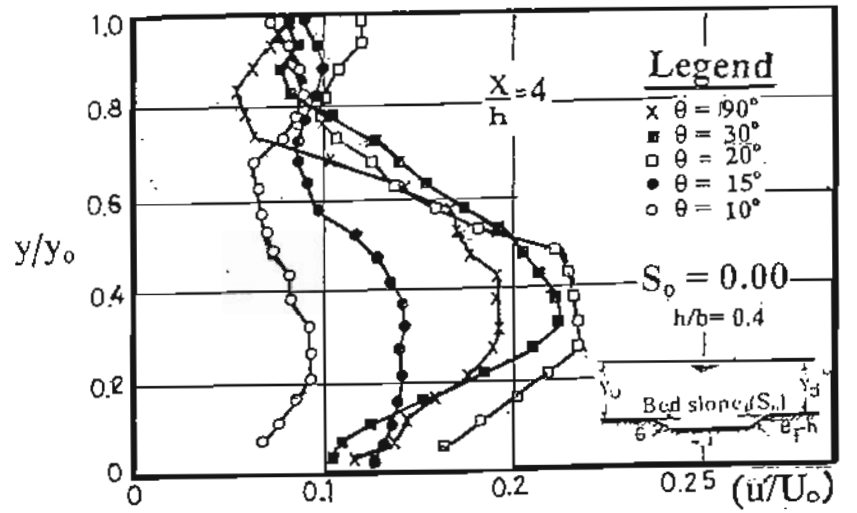

Fig. 14 Variation of streamwise turbulence intensities $\acute{u}/U_o$ with y/y_o at x/h=4 for different angles

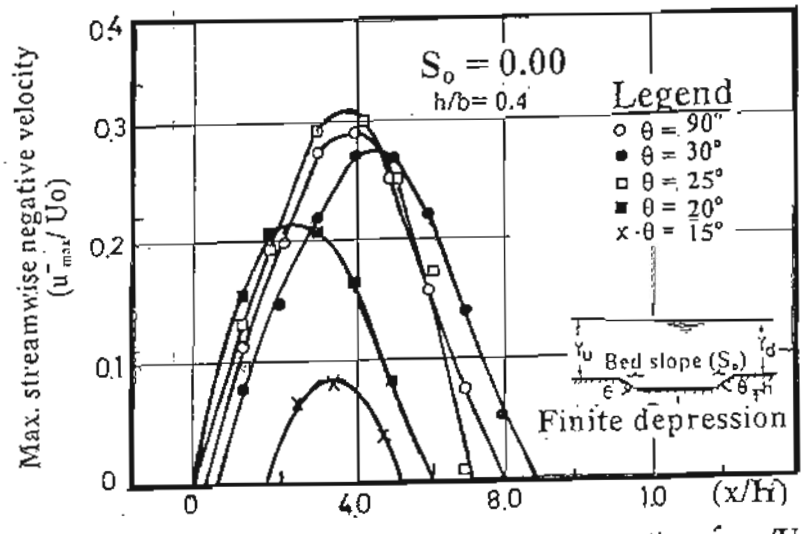

Fig. 13 Variation of max. streamwise negative $\acute{u}_{max}/U_o$ Along the centerline for different angles

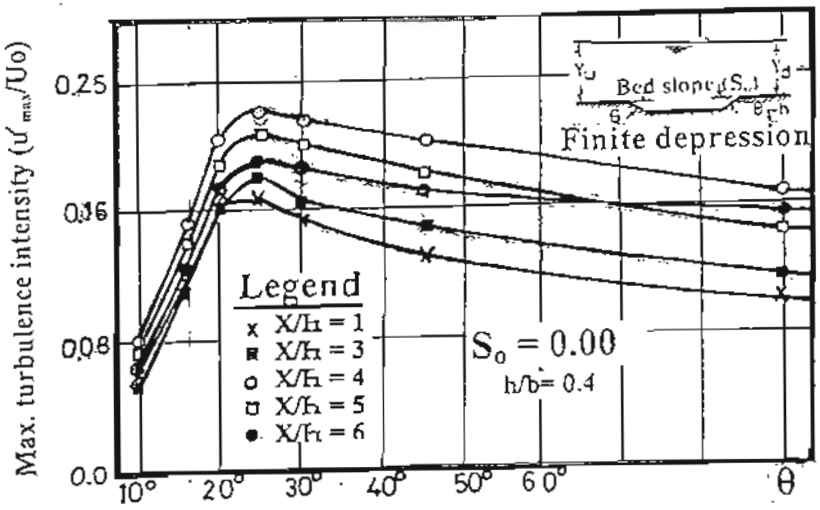

Fig. 15 Variation of max. streamwise turbulence Intensities $\acute{u}_{max}/U_o$ as a function of depression angle at different positions

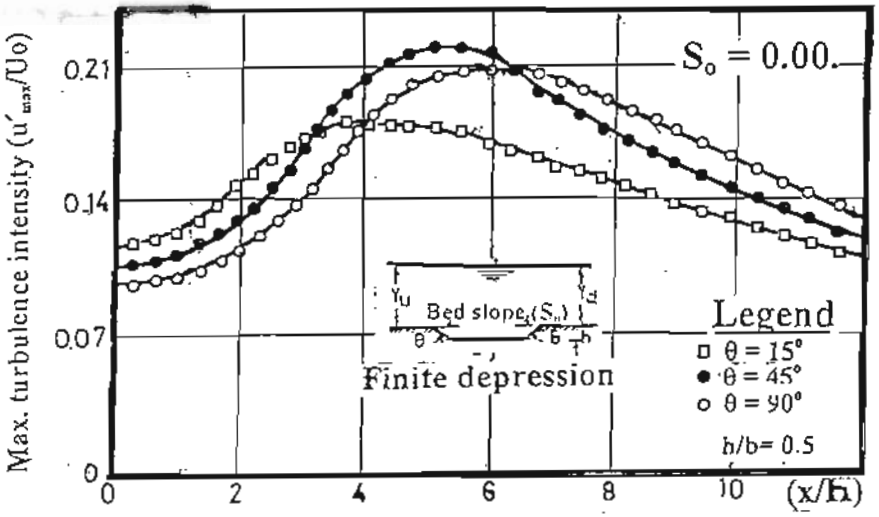

Fig. 16 Variation of max. streamwise turbulence intensities u_{max}/U_o along the centerline for different angle

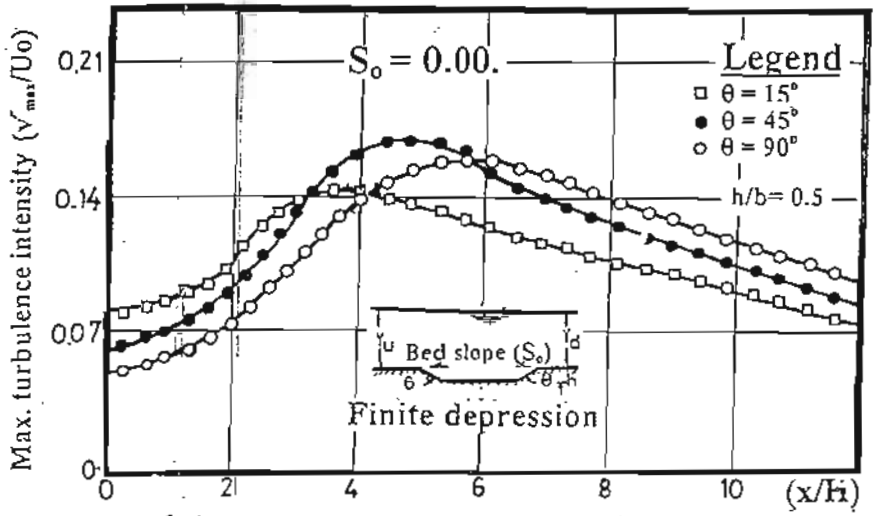

Fig. 17 Variation of max. vertical turbulence intensities v_{max}/U_o along the centerline for different angles

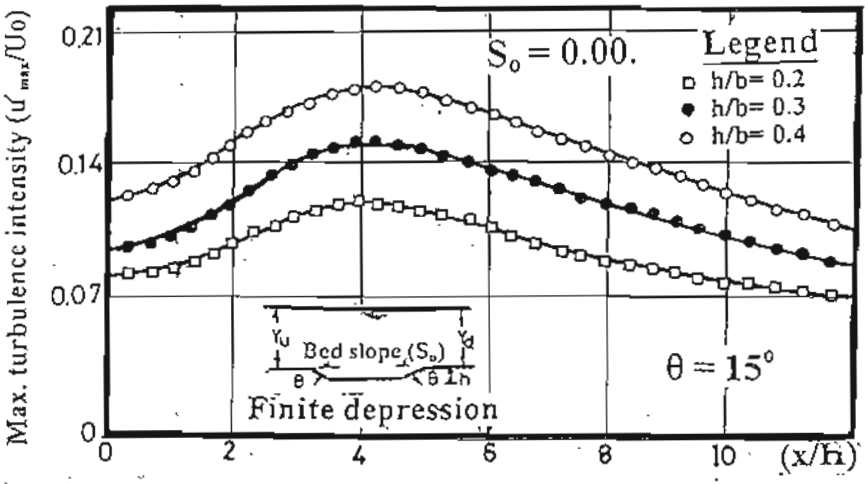

Fig. 18 Variation of max. streamwise turbulence intensities $\acute{u}_{max}/U_o$ along the centerline for different relative height h/b

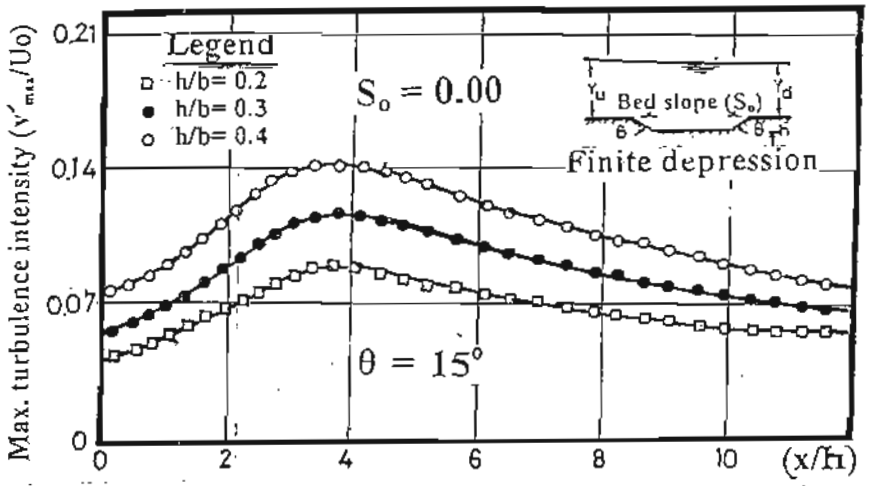

Fig. 19 Variation of max. vertical turbulence intensities $\acute{v}_{max}/U_o$ along the centerline for different relative height h/b